THE ADDITIVE CORRECTION MULTIGRID METHOD FOR UNSTRUCTURED GRIDS

Susie Cristine Keller
susie@sinmec.ufsc.br

Jonas Cordazzo
jonas@sinmec.ufsc.br

Pedro H. Hinckel
phhinckel@sinmec.ufsc.br

Clovis R. Maliska
maliska@sinmec.ufsc.br

SINMEC – Laboratory of Numerical Simulation in Fluid Dynamics and Computational Heat Transfer
Dept. of Mechanical Engineering
Federal University of Santa Catarina
Postal Office Box 476
Zip Code: 88040-900 Florianopolis, SC, Brazil

Abstract. *This paper shows a study using the Additive Correction Multigrid (ACM) method pointing out and its main features. The motivation of ACM, as other multigrid methods, is to solve efficiently a large set of algebraic equations resulting from the discrete approximation of differential equations. It is demonstrated that ACM accelerates a solution of equations set and reduces the complexity and the computational cost because the discretization is made only in fine grid equations. It is a conservative method because the coefficients in the coarse grid equations are formed by the summation of the coefficients in the fine grid equation. Another ACM advantage is the use of the adaptive agglomeration of cells, which diminishes the anisotropy of the coarser grid coefficients, preventing the convergence rate stagnation. Besides showing the Additive Correction strategy, we perform a parametric study of the factors which influence on its performance, namely the type of multigrid cycle used and agglomeration scheme adopted, among others. The agglomeration algorithm is also outlined and can be applied to any type of mesh, structured or not.*

Keywords: *Additive Correction Multigrid (ACM), Agglomeration scheme, Multigrid cycles, Element- based Finite Volume Method, Unstructured grids.*

1. INTRODUCTION

In recent years, multigrid methods have been receiving considerable attention to reduce drastically the computation time. The basic idea of a multigrid strategy is to use a sequence of grids together with classical iterative solvers to smooth the high-frequency modes of the error for each grid. On the finest (original) grid, the high-frequency modes of the error are effectively reduced, but the low-frequency modes are difficult to remove, since they would require coarser grids to attain this goal. With a minimal computational effort, multigrid methods can eliminate low-frequency modes of the error solving the coarse grid error approximation, which is much less expensive than solve the original equations.

The objective of this article is to show and to analyze one type of multigrid scheme, the Additive Correction Multigrid method (Hutchinson and Raithby, 1986), simply called here as ACM. In ACM, the coarse grid-equations are generated by the summation of the finer grid equations. Once the solutions on the coarser grid are obtained, they are simply added to the solution on the finer grid. Thus, interpolation or extrapolation operators, commonly used by multigrid classical methods, are not required and the conservation principle is satisfied at all grid levels.

It is also analyzed the effect that the anisotropic coefficients have on the ACM method. Studies of iterative methods have shown that their performance decreases when the coefficients of the linear equation become highly anisotropic (Elias et al., 1997). This anisotropy of coefficients causes different timescales for propagation of information, which dramatically affect the convergence behavior. Thus, the type of adaptive agglomeration, which is provided by the ACM method turns the multigrid method more efficient because the variation in timescales for the propagation of information on a coarse-grid cell is reduced. The procedure consists in adding fine-grid cells with small transport timescales.

In order to evaluate the potentialities of the ACM method, in this work it is shown some heat conduction problems, whose differential partial equations are discretized using the conventional Finite Volume Method (FVM) and the Element-based Finite Volume Method (EbFVM). By conventional Finite Volume method it is meant the method which uses the control volume coincident with the element and, usually, with structured grids. The EbFVM, used here deals with unstructured grids and are suitable to be used with triangular as well as quadrilateral elements.

2. THE ADDITIVE CORRECTION MULTIGRID METHOD

In the ACM method the discretization is made only in the finest grid. The role of the coarse grid equations, which are formed by adding the fine-grid equations, is to generate corrections to the fine grid solution in order to asserting integral conservation over blocks of control volumes. ACM determines these constant corrections in coarse grid cells by forcing the sum of residuals be zero after the correction is applied.

Initially we show that the system of equations to be solved can be written in the common form as

$$A_i \phi_i = \sum_{nb} A_{nb} \phi_{nb} + b_i \,, \tag{1}$$

where A_i is the central coefficient of the control volume i considered in the discrete equation for ϕ, A_{nb} are the coefficients connecting the control volume i to the neighbors control volumes, b_i is the source coefficient and ϕ is the solution. The coefficients of Eq. (1) can be obtained by applying Finite Volume or Finite Difference techniques to either structured or unstructured grids (Maliska, 2004).

Thus, it is defined a correction equation that has the role of adding coarse-grid corrections (ϕ^*) to the best estimate of ϕ on the fine grid, as

$$\widetilde{\phi}_i = \phi_i + \phi^*_{I,i}, \tag{2}$$

where $\widetilde{\phi}_i$ is the improved solution in each cell and $\phi^*_{I,i}$ is the correction related to all volumes that lie within the *I* block. The *I* block contains the *i* control volumes, as shown in Fig. (1).

Requiring that the residual be zero for the corrected solution, one obtain the linear system for $\phi^*_{I,i}$

$$A^*_p \phi^*_p = \sum_{nb} A^*_{NB} \phi^*_{NB} + b^*_p, \tag{3}$$

where

$$b^*_p = \sum_{i,I} r_i ,$$

$$A^*_P = \sum_{i,I} A_{i,p} - \sum A_{nb} ,$$

$$A^*_{NB} = \sum_{i,I} A_{i,nb} .$$

Thus, $\sum A_{nb}$ denotes the connection among the volumes inside the same block and $\sum_{i,I} A_{i,nb}$ represent the connection among volumes of neighbor blocks. Details of the ACM method can be found in (Hutchinson and Raithby, 1986 **)** and in (Maliska, 2004).

Equation (3) must be solved in order to obtain the correction $\phi^*_{\mathrm{I,I}}$. This correction is added to each ϕ value of control-volumes that lie within the *I*-block. Thus, the improved estimate $\widetilde{\phi}_i$ is obtained.

Using the ACM method, there are no further decisions to be made related to the boundary conditions, transfer of residuals or interpolation of variables. These choices are constrained, because ACM requires that the integral conservation over each coarse grid control volume be satisfied.

In the next section it is presented the adaptive agglomeration scheme, which improves even more the performance of the ACM method.

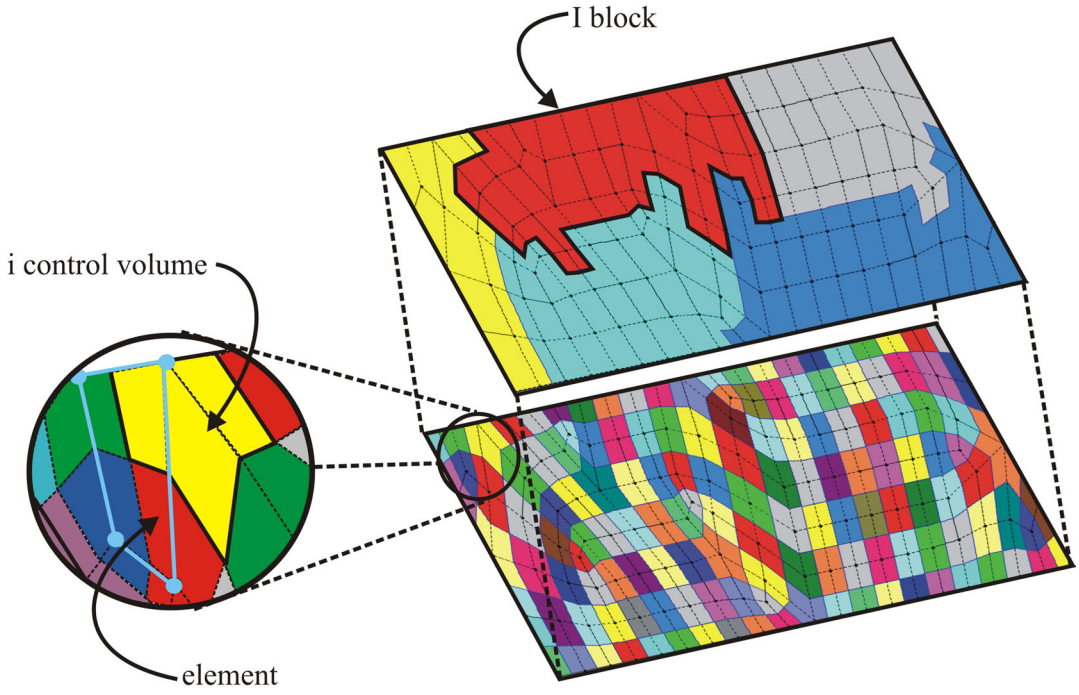

Figure 1. Example of an adaptive agglomeration in unstructured grid.

2.1 Adaptive agglomeration scheme

The nature of the coefficients in the fine grid equations can strongly affect the convergence behavior of an iterative solver. This occurs because the anisotropy of the coefficients causes different timescales for propagation of information. Therefore, an adaptive agglomeration method based on the fine grid coefficients and on the anisotropic degree should be usedin order find the new corse grid.

As shown in Elias (1993), the coefficient $a_{i,j}$, for a advection/diffusion problem, which represent the influence of a neighbor cell node j on the cell node i, is given by:

$$a_{i,j} = \frac{\Gamma_{i,j}\Delta s}{\Delta n} + \max\left(-\rho_{i,j}u_m\Delta s, 0\right), \tag{4}$$

where $\Gamma_{i,j}$ is the diffusivity at the face, Δs is the width of the face between the nodes, Δn is the distance between the nodes, $\rho_{i,j}$ is the density at the face and u_m is the face normal velocity.

Thus the natural timescale $\tau_{i,j}$ for a perturbation in ϕ to travel from the neighbor node j to the cell node i is inversely proportional to the influence coefficient between i and j:

$$\tau_{i,j} = \frac{\rho_{i,j}\Delta s\Delta n}{a_{i,j}}. \tag{5}$$

For iterative methods, like Gauss-Seidel and others, there is a time step over which the solution at node i is advanced in one iteration, namely $\Delta t_i = min(\tau_{i,NB})$. Thus, the performance of iterative solver degrades when there is a high difference between the implied solver time step and the timescales to propagate the information between nodes. In order to accelerate the convergence of the discrete linear equations set solution, we can generate a

coarse grid equations set by adding cells to reduce the differences between the largest and smallest transport time scales. This is the principle of adaptive agglomeration (Elias, 1993).

The agglomeration scheme begins with a single fine grid cell and through a set of rules it determines which of the neighbors should be included in the new coarse cell. This is done until the coarse cell reaches the desired size, or there are no more neighbors to be added.

The nomenclature of a family tree (Elias et al, 1997) is now considered. We call the fine grid cell, whose neighbors are being examined, as the parent, and its neighbors included in the same coarse cell as its children. The current parent's parent is known as the grandparent. We can see the agglomeration process systematized in Fig. (2) and (3).

Figure 2 shows the agglomeration process in a general manner. The process starts with the choice of the new father. To simplify the process, the first parents are selected in the same sweep order of the iterative solver. Then the possible son and its best neighbor are searched in order to the rule two can be tested. This agglomeration rule states that a cell is excluded if the interface timescale is very large. The concept of what would be "large" is defined relative to all other timescales which affect the cell in question. A possible child can be agglomerated with the parent if the coefficient that connects the parent with the child is of the same order or larger than the coefficient that connects the possible child with its neighbors. If this rule is satisfied, the first agglomeration in the new block is made. Then, if the agglomerated cells number in block did not reach the defined cells number per block, the agglomeration process continue.

Following the scheme described in Fig (2), we can see that the searching for a best son can be done according to the procedure of Fig (3). This figure depicts a function which returns a best son, if it exists. This best son is the cell with larger connection with father the cell and with good geometric position in the block. The last characteristic means a cell which has neighbors in block besides the parent. There are three possibilities of choosing the best son, as can be seen in Fig. (3). Then, the chosen cell is tested in rule one, which states that the coefficient that connects the parent with the neighbor must be of the same order or larger than the coefficient that connects the parent with the grandparent. If this rule is satisfied, the best son exists and it is returned by the function. Thus, this procedure continues until the coarse cell reaches the specified size or there are no more neighbors, which satisfy the rules, to be added. Then a new father is chosen and the agglomeration process continues until the last cell is examined.

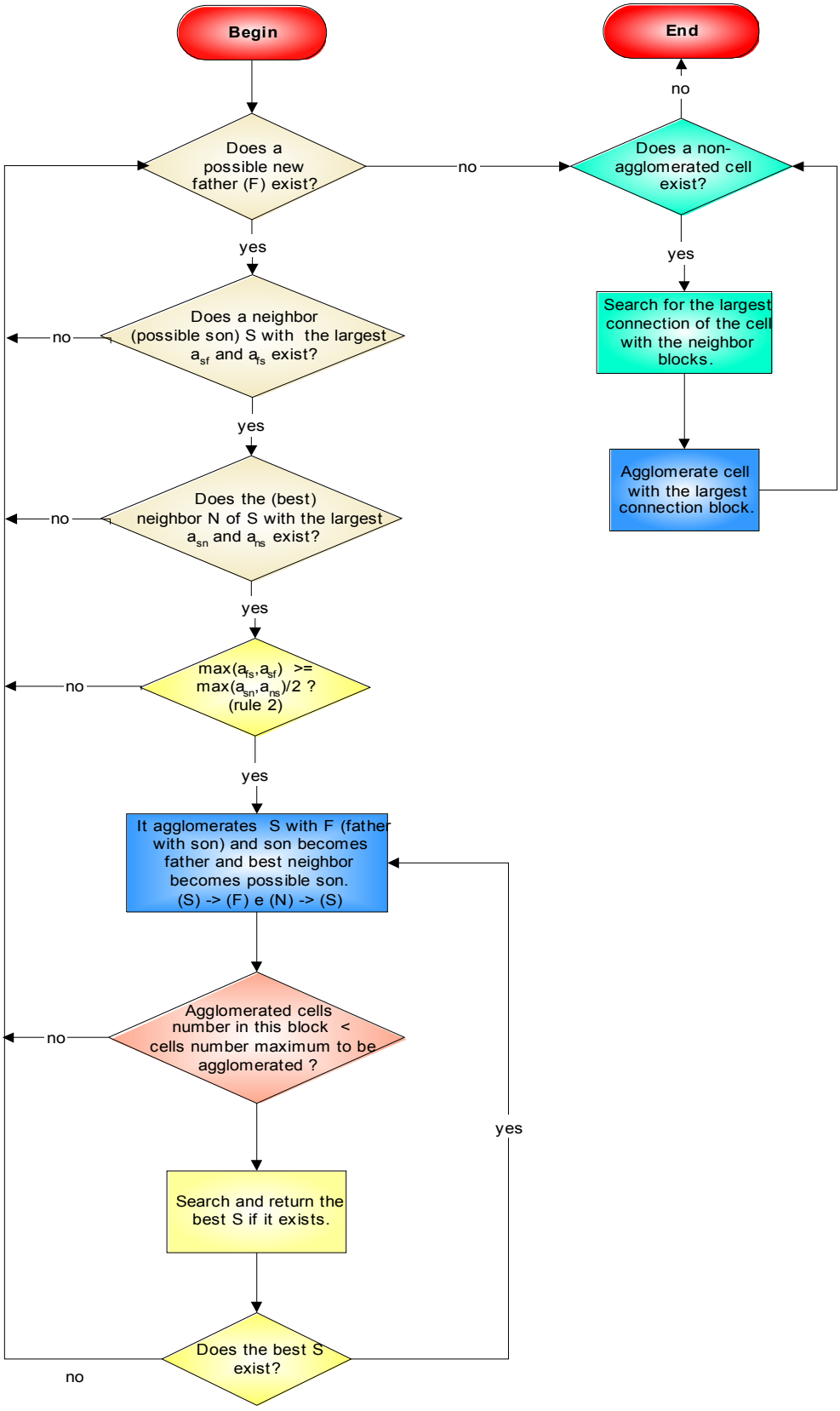

Figure 2. Flowchart of adaptive agglomeration scheme.

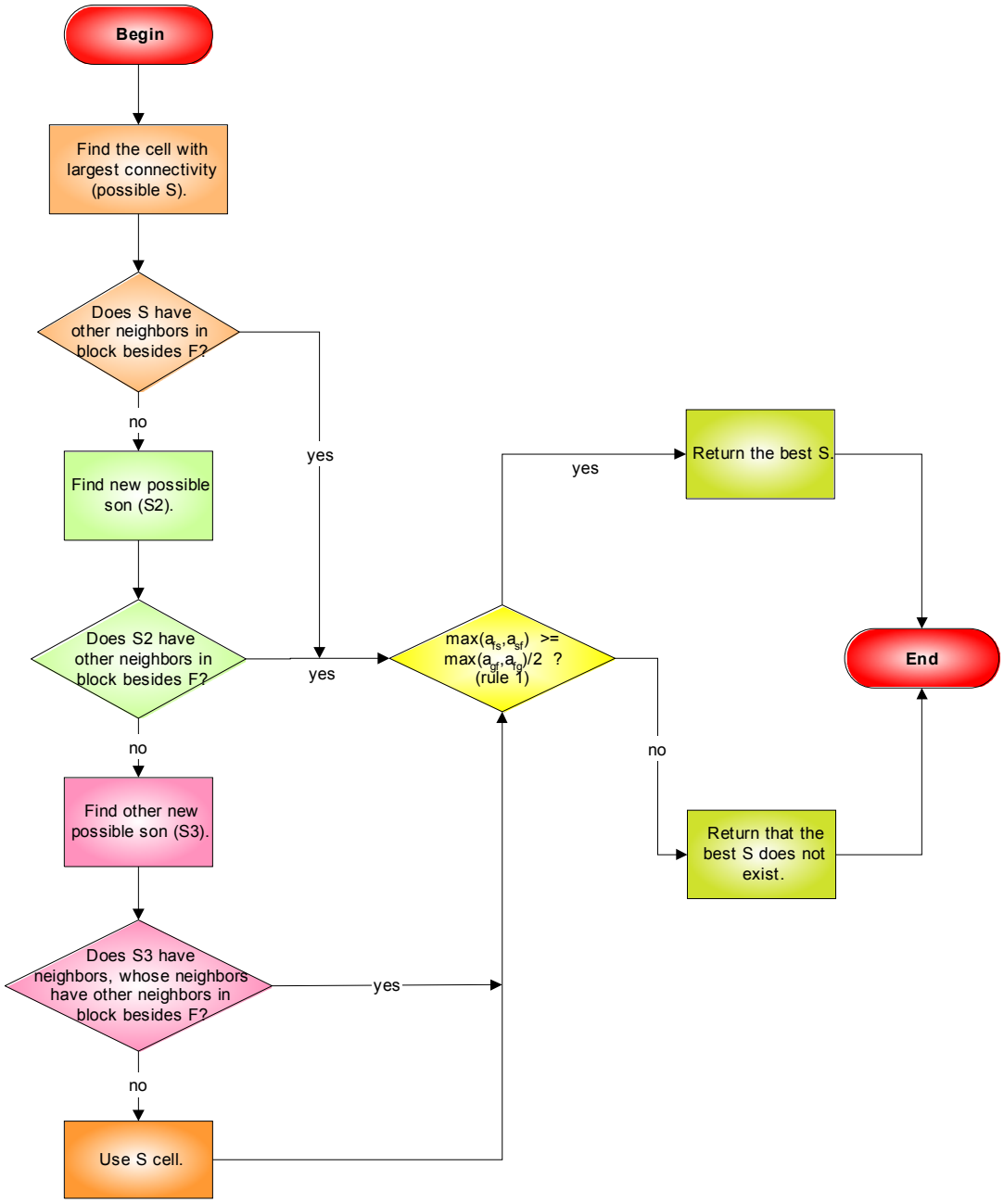

Figure 3. Procedure for searching the best son.

It is possible that there are remaining cells in the fine grid without any neighbor that can be used as child. To eliminate wasted computational effort with those single cells, any parent cells which do not have children are forced to join the coarse grid cell of its most strongly connected neighbor. This can be seen in Fig. (2) also.

The next item presents several multigrid cycles that can be used, showing their main features.

2.2 Multigrid cycles

The multigrid principle is to solve the discrete linear equations in several grids reducing all frequency modes of the error whose wave-length is of the same order as the grid spacing. As already stated, on the finest (original) grid, the high-frequency modes of the error are

effectively reduced, but the low-frequency modes are difficult to remove, since they would require coarser grids to attain this goal. The manner how the coarser grids are used configures the type of the cycle. The most common cycles related in literature are V, W and F cycles (Trottenberg, 2001). In the V cycle the work to solve the linear equation set is made in fine and coarser meshes in equal ratio. In W and F cycles, on the other hand, the most of the work is made in the coarser grids. These multigrid cycles with several levels can be seen in Fig. (4).

Another technique that has been related in the literature (Trottenberg, 2001) is the full multigrid technique (FMG). The main idea of FMG is to use coarse grids to obtain improved initial approximation for the fine grid problems. This technique, which can be applied to any type of cycle, can be considered the most effective way of accelerating the multigrid convergence, because the discrete linear system is solved only in the ascent direction of the cycle used. The contribution of the multigrid in that direction is the most important. For this reason, FMG is used in all examples in this paper.

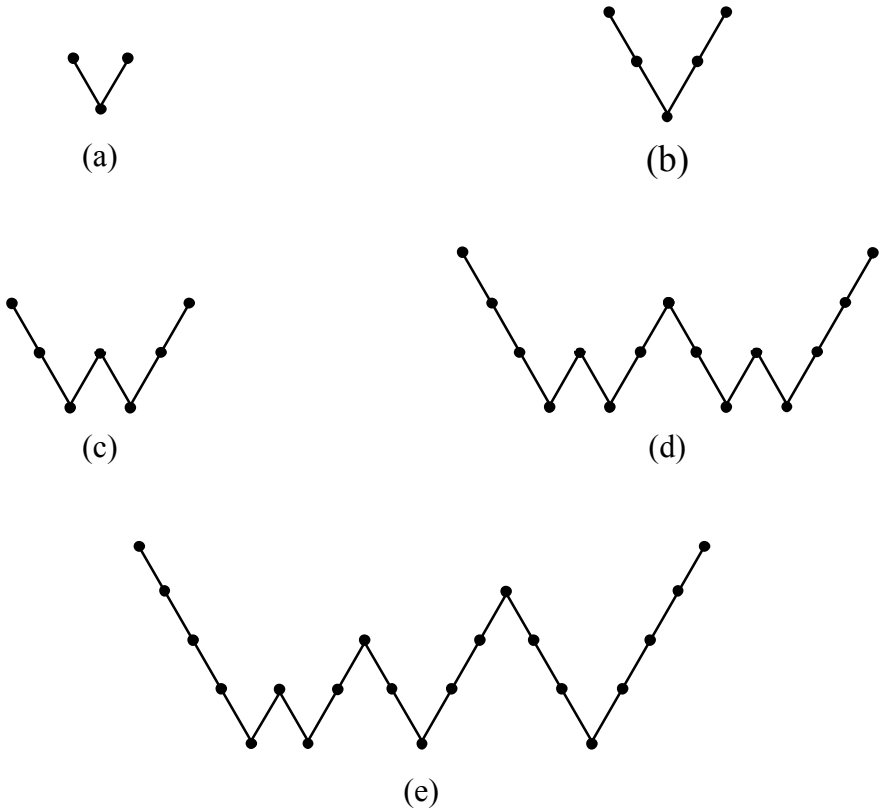

Figure 4. Multigrid cycles: V with (a) two and (b) three grid levels, W with (c) three and (d) four grid levels and (e) F with five grid levels.

In next section, it is shown the method used to discretize the differential equation in most problems analyzed in this paper.

3. ELEMENT-BASED FINITE VOLUME METHOD (EbFVM)

In a finite volume methodology the computational domain is covered by non-overlaping control-volumes where the balances are made. In the EbFVM the element concept and their geometric representation inherited from the finite element method is utilized, and its definition precedes the creation of the control volume. Figure (5) shows an example of an

EbFVM grid, emphasizing the differences between grid elements (quadrilaterals) and control-volumes (built around the grid nodes).

The control volumes are created by the method of the medians, which consists of joining the center of the elements to their medians. The resulting control volume is formed by portions (sub-control volumes - scv) of neighboring elements. The integration of the conservation equation over the control volume interfaces is evaluated at the integration points, as shown in Fig. (5).

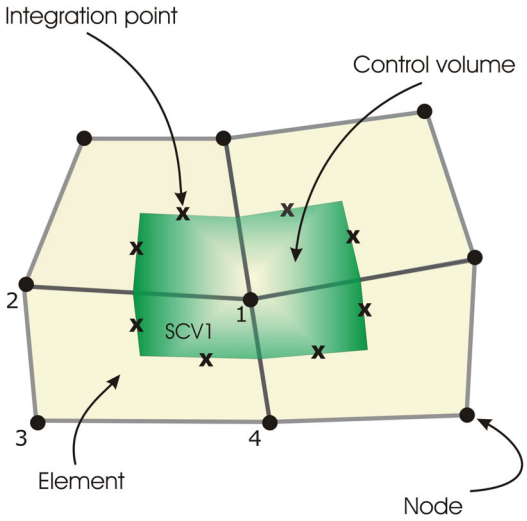

Figure 5. Example of a grid utilized by EbFVM.

Each element in a grid is treated identically in the EbFVM, no matter how distorted the element may actually be in terms of global coordinates. This is possible due to the use of the local coordinates. In Fig. (6) one can see an example of a transformation of an element from the physical plane *(x,y)* to the transformed plane *(ξ, η)*, whose axes vary $-1 \leq \xi \leq 1$ and $-1 \leq \eta \leq 1$.

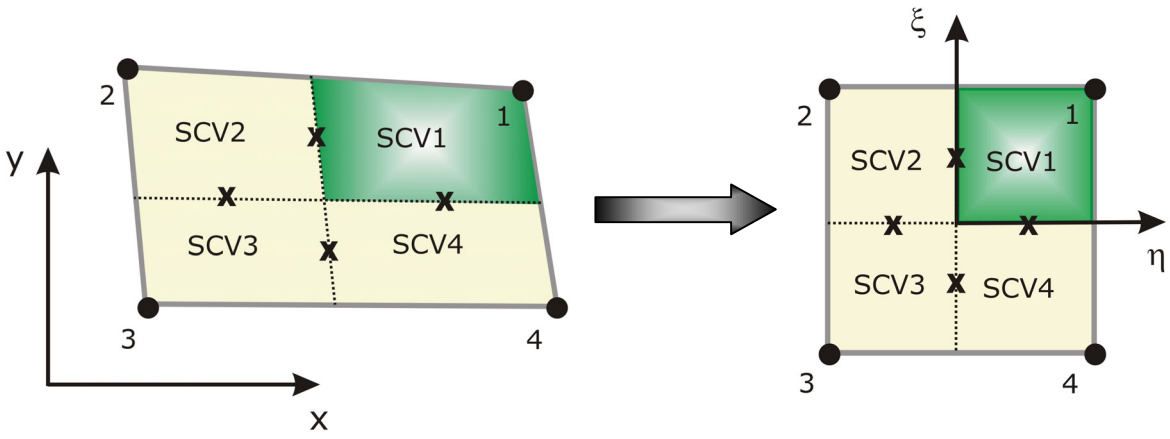

(a) (b)

Figure 6. Physical (a) and transformed (b) domains.

The EbFVM will be used in this work to solve simple heat transfer problems, in order to pointing out the potentialities of the ACM algebraic multigrid method. The steady-state heat conduction equation, without heat generation is given as

$$\frac{\partial}{\partial x_j}\left(k\frac{\partial T}{\partial x_j}\right)=0\,, \tag{6}$$

where k is a thermal conductivity, x_j are the global coordinates and T is the temperature.

Integrating the equation for an arbitrary control volume, it results in:

$$\sum_{ip}\left(k\frac{\partial T}{\partial \vec{n}}\right)_{ip}\Delta s_{ip}=0\,, \tag{7}$$

where ip are the integration points, $\vec{n}$ is the normal vector and Δs is the face area.

The shape functions, which are used to describe the variation of the global coordinates within the element, can be used also to describe the variations of T within the element. Thus:

$$T(\xi,\eta)=\sum_{i=1}^{4}N_i(\xi,\eta)T_i\,, \tag{8}$$

where the shape functions N_i for quadrilaterals elements are defined by:

$$N_1(\xi,\eta)=\frac{1}{4}(1+\xi)(1+\eta), \tag{9.1}$$

$$N_2(\xi,\eta)=\frac{1}{4}(1-\xi)(1+\eta), \tag{9.2}$$

$$N_3(\xi,\eta)=\frac{1}{4}(1-\xi)(1-\eta), \tag{9.3}$$

$$N_4(\xi,\eta)=\frac{1}{4}(1+\xi)(1-\eta). \tag{9.4}$$

and the nodal i coordinates x_i and y_i can be write by:

$$x(\xi,\eta)=\sum_{i=1}^{4}N_i(\xi,\eta)x_i\,, \tag{10.1}$$

$$y(\xi,\eta)=\sum_{i=1}^{4}N_i(\xi,\eta)y_i\,. \tag{10.2}$$

Therefore, the derivatives of T in Eq. (7) can be determined as

$$\left.\frac{\partial T}{\partial x}\right|_{\xi,\eta}=\sum_{i=1}^{4}\left.\frac{\partial N_i}{\partial x}\right|_{\xi,\eta}T_i\,, \tag{11.1}$$

$$\left.\frac{\partial T}{\partial y}\right|_{\xi,\eta}=\sum_{i=1}^{4}\left.\frac{\partial N_i}{\partial y}\right|_{\xi,\eta}T_i\,, \tag{11.2}$$

where the N derivatives is given by

$$\frac{\partial N_i}{\partial x} = J\left[\frac{\partial N_i}{\partial \eta}\frac{\partial x}{\partial \xi} - \frac{\partial N_i}{\partial \xi}\frac{\partial x}{\partial \eta}\right], \tag{12.1}$$

$$\frac{\partial N_i}{\partial y} = J\left[\frac{\partial N_i}{\partial \xi}\frac{\partial y}{\partial \eta} - \frac{\partial N_i}{\partial \eta}\frac{\partial y}{\partial \xi}\right], \tag{12.2}$$

where the Jacobian is given by

$$J = \left[\frac{\partial x}{\partial \xi}\frac{\partial y}{\partial \eta} - \frac{\partial x}{\partial \eta}\frac{\partial y}{\partial \xi}\right]^{-1}, \tag{13}$$

and the derivatives of the shape functions related to ξ and η, in turn, are

$$\frac{\partial N_i}{\partial \xi} = \frac{\partial N_i}{\partial x}\frac{\partial x}{\partial \xi} + \frac{\partial N_i}{\partial y}\frac{\partial y}{\partial \xi}, \tag{14.1}$$

$$\frac{\partial N_i}{\partial \eta} = \frac{\partial N_i}{\partial x}\frac{\partial x}{\partial \eta} + \frac{\partial N_i}{\partial y}\frac{\partial y}{\partial \eta}. \tag{14.2}$$

The derivatives in Eq. (7) can, therefore, be substituted by Eqs. (11) to obtain the linear system for discrete temperature field in the form

$$A_i T_i = \sum_{nb} A_{nb} T_{nb} + b_i \tag{15}$$

The above linear system will be solved using the ACM approach. More details involving the deduction of EbFVM discretized equations can be found elsewhere (Raw, 1985; Maliska, 2004)

4. RESULTS

Three example problems will be presented to demonstrate the efficiency of the ACM method with the agglomeration scheme. The results are obtained using two different solvers: Gauss-Seidel and ACM with different number of levels of agglomeration and cycles. In the last level, the coarsest one, equations were solved with a direct-LU solver, while the other coarse levels were solved using Gauss-Seidel. The maximum allowed residue adopted was 10^{-5}. We use the V, W and F cycles in all cases analyzed here.

The first example is a square 2D heat conduction problem with anisotropic regions. The geometry and the boundary conditions of this problem are presented in Fig. (7). The discretization was made using the conventional FVM (Maliska, 2004) with a grid of 20x20 regular volumes.

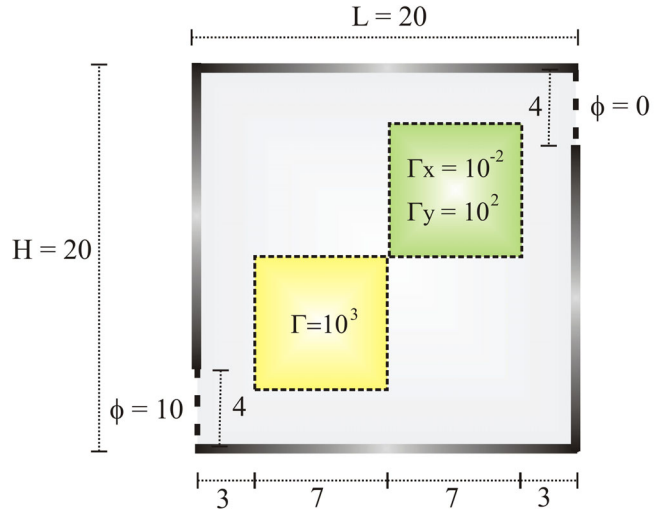

Figure 7. Geometry of the diffusion problem.

The agglomeration of the volumes was performed using six fine grid cells per new coarse cell, which result in the meshes shown in Fig. (8).

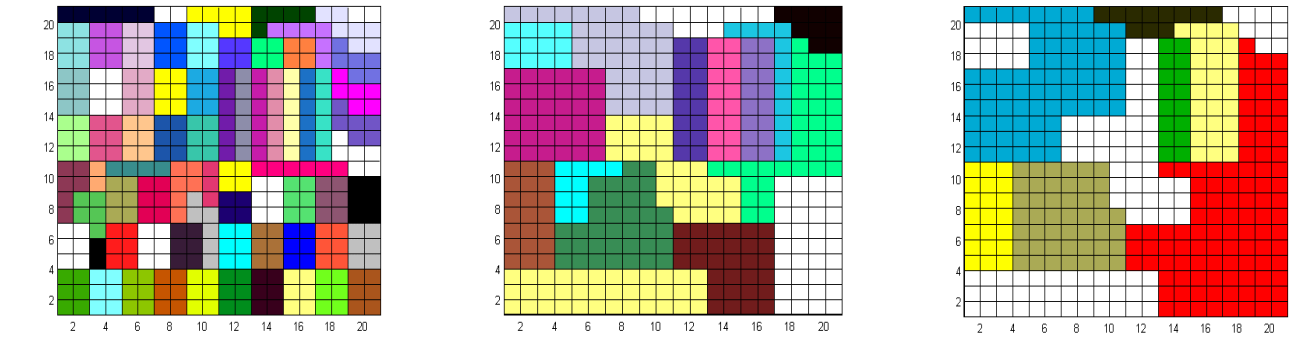

(a) (b) (c)

Figure 8. Different levels of agglomeration.

We can see that in the first coarse grid, Fig. (8a), the cells generated are reasonably regular. The agglomeration occurs in the direction of a small transport timescales (high diffusivities) in anisotropic zones. In the second and third agglomerations, Fig. (8b) and (8c), coarser blocks continue keeping a good separation of the three diffusivity zones. This behavior was also verified in the work of Elias et al. (1997), and it was expected, since the same basic ideas concerning the agglomeration scheme is used here.

For this problem, the three multigrid cycles tested had the same computational time. Probably, it occurs because the grid utilized is coarse. We opted to present only the ACM V cycle in Fig. (9).

Thus, Fig. (9) shows the comparison between the convergence behaviors on this diffusion problem obtained by Gauss-Seidel method and ACM method with different number of agglomeration levels. It is shown that ACM method is more efficient than Gauss-Seidel, as expected. Tests show that this difference in total CPU time tends to grow up when the mesh is more refined. It demonstrates that the adaptive agglomeration, which joins cells with small transport time scales, is a promising technique. In this case, the multigrid with three levels demonstrates to be the best in residual reduction.

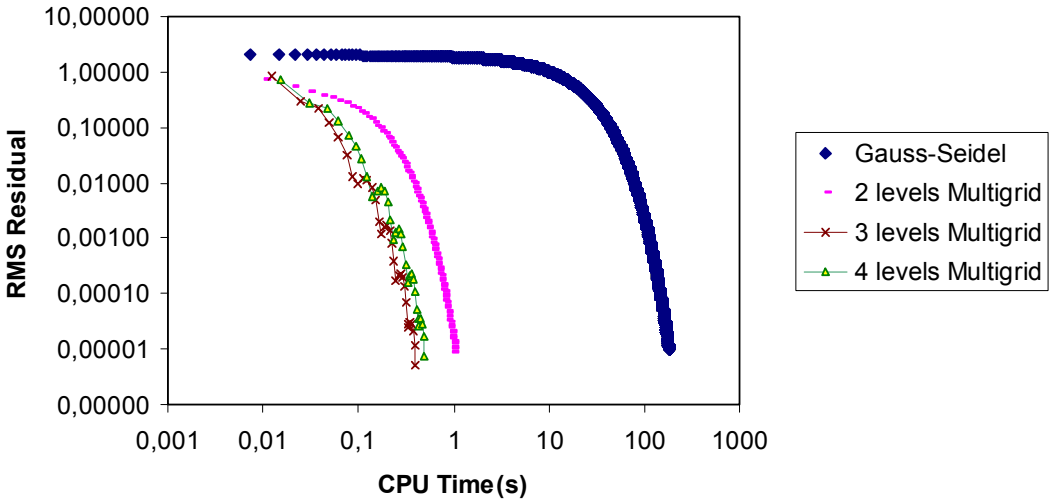

Figure 9. Residual reduction with time.

The second problem considered is a diffusion problem with x-boundaries of the domain insulated and the y-boundaries partly insulated, as represented in Fig. 10. The EbFVM was used for discretizing this problem because it treats the grids in an unstructured fashion, even though it is used here grids geometrically structured with 1024, 4096 and 16384 nodes or control-volumes equally in both x and y directions. Because of the problem geometry, the coefficients related to nodes in the interior of domain are greater in the y direction than in x direction. The agglomeration is always made in the direction of the greater coefficients.

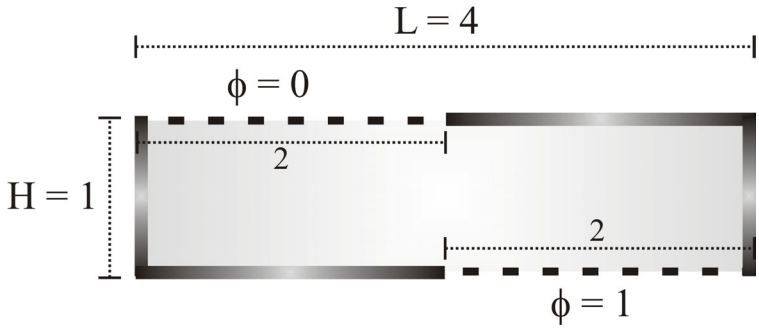

Figure 10. Geometry of the second example problem.

In Fig. (11), the total CPU time needed to reduce the RMS residual to a pre-determined value (in this case 10^{-5}) obtained by different methods is presented. According to this figure, in the 1024-node grid, ACM with V, W and F cycles and Gauss-Seidel converged to the desired solution in the same computational time. It occurs because the coefficients are large in the y direction and the effect of the Dirichlet boundary conditions is rapidly transmitted to interior of domain. Thus, the residue to be eliminated in the x direction is small and Gauss-Seidel is sufficient to solve this diffusion problem.

However, in 4096 and 16384-node grid, ACM has a significant computational time reduction, as shown also in Fig. (11). Due to the increasing of the number of nodes in the y direction, as expected, the propagation of the Dirichlet conditions has become slower in the y direction when the Gauss-Seidel solver is used. Thus, the ACM is more efficient for using an adaptive agglomeration, which facilitates the travel of the information into the interior of

domain. In these cases, we can see a small difference among the multigrid cycles V, W and F. More specifically, in 16384-node grid, it can be seen clearly a difference among the three cycles, where V cycle was the best, followed by F cycle and then the W cycle.

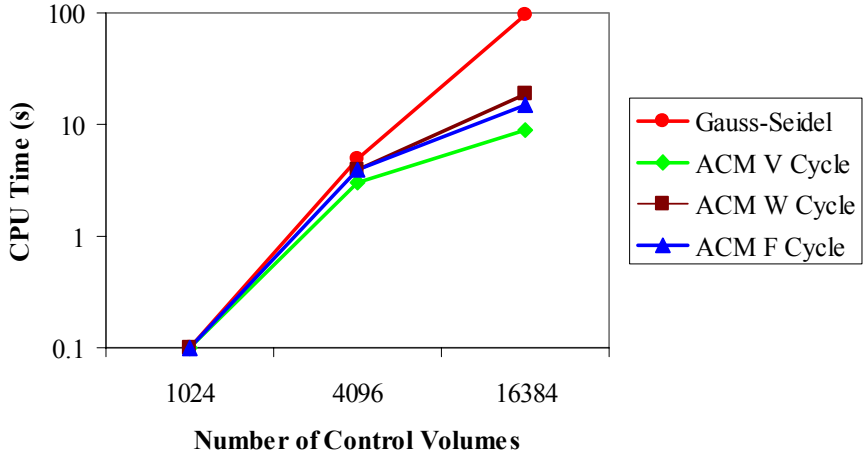

Figure 11. Residual reduction with time in the second problem.

The third example is similar to the second one, except for the boundary conditions on x and y coordinates that are interchanged (Fig. 12). In this example, the information about the boundary conditions is transmitted mainly in the direction of smaller coefficients, so we expect a larger computational effort required for Gauss-Seidel to reach the convergence.

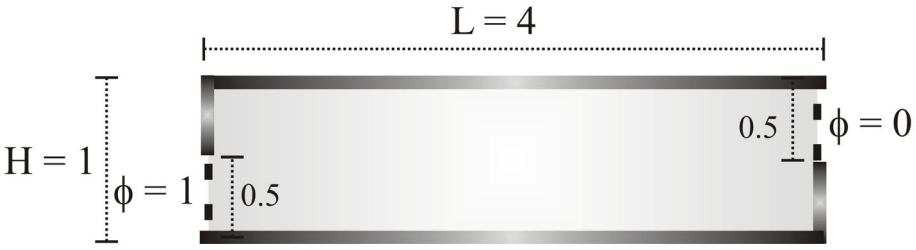

Figure 12. Geometry of the third example of diffusion problem

In Fig. (13), we can see the high computational time gain of ACM over Gauss-Seidel solver. It occurs because the Dirichlet boundary conditions are prescribed in the weak coefficient direction, as already stated. Thus, Gauss-Seidel propagates the boundary condition information in this direction one node per iteration, while ACM propagates the information over the whole domain in only one iteration. As before, Fig. (13) shows that the number of grid nodes grow up the efficiency of ACM in comparison with Gauss-Seidel. The computational time obtained by these three multigrid cycles was very similar one to another in this example.

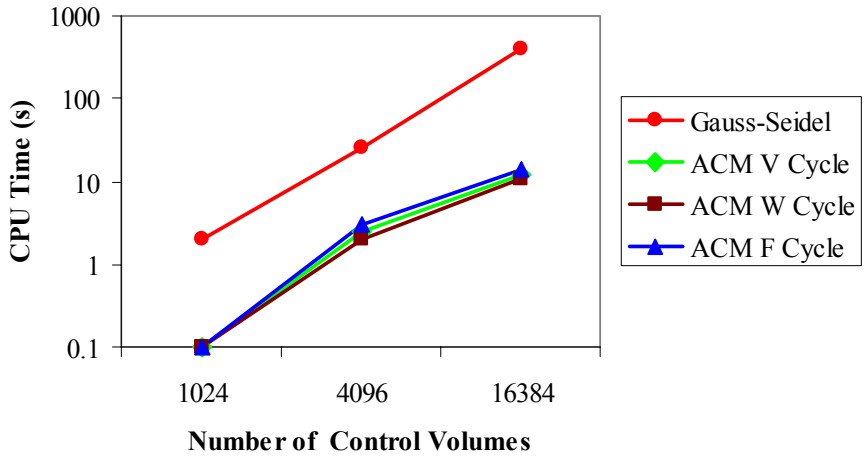

Figure 13. Computational effort in the third test problem.

5. CONCLUSIONS

This paper has outlined some of the ACM main features. It was shown that the performance of iterative solvers tends to degrade when the matrix coefficients are anisotropic, or the number of equations becomes large. Therefore, agglomeration techniques based only on geometric consideration is not suitable. Thus, the ACM main feature, the adaptive agglomeration, is very appropriate because it joins cells in order to eliminate small transport time scales.

A study was done to examine the multigrid cycles V, W and F. Using unstructured meshes, it was difficult to show which cycle is the fastest, because all cycles had a similar computational time. As one can see in Figs. (11) and (13), the multigrid cycle efficiency depends on the problem. Thus a more effective analysis must to be done. We have a feeling that the differences in CPU gain between the results shown in this paper and the results presented in the literature (Elias, 1993) are due to the use of unstructured grids and the EbFVM for discretizing differential equations. The use of EbFVM with quadrilateral elements results in control volumes that have eight neighbors instead of only four neighbors as in structured quadrilateral meshes. This fact can result in an agglomeration scheme not so appropriate to unstructured grids.

Despite this fact, the ACM method has been shown to be better than Gauss-Seidel solver, diminishing considerably the solution times.

These initial tests are strongly encouraging. More analyses in unstructured meshes must be done. Efforts are going on foreseeing the application of this principle to a coupled linear equation system, aiming also the development of new features in the adaptive agglomeration scheme.

REFERENCES

Elias, S. R., 1993. *Enhancements to Additive Correction Multigrid*. Master thesis, University of Waterloo/Canada.

Elias, S.R., Stubley, G.D., Raithby, G.D., 1997. An Adaptative Agglomeration Scheme for Additive Correction Multigrid. *International Journal of Numerical Methods in Engineering*, Vol. 4 (5), pp.887-903.

Hutchinson, B. R., Raithby, 1986. A Multigrid Method based on the Additive Correction Strategy. *Numerical Heat Transfer*, Vol. 9, pp. 511-537.

Maliska, C. R., 2004. *Transferência de Calor e Mecânica dos Fluidos Computacional*. Ed. LTC.

Maliska, C. R., 2002, A General View of Constructing Finite Volume Methodologies for Fluid Flow Simulations. *III Escola de Primavera de Transição e Turbulência*, pp. 345-364.

Raw, M. J., 1985. *A New Control-Volum-Based Finite Element Procedure for the Numerical Solution of the Fluid flow and Scalar Transport Equations*. Doctor thesis, University of Waterloo/Canada.

Trottenberg, U., Oosterlee, C., Schüller, A., 2001. *Multigrid*. Academic Press.